AGU PUBLICATIONS

Water Resources Research

RESEARCH ARTICLE
10.1002/2014WR015685

Modeling spatiotemporal impacts of hydroclimatic extremes on groundwater recharge at a Mediterranean karst aquifer

Andreas Hartmann[1,2], Matías Mudarra[3], Bartolomé Andreo[3], Ana Marín[3], Thorsten Wagener[1], and Jens Lange[2]

[1]Department of Civil Engineering, University of Bristol, Bristol, UK, [2]Institute for Hydrology, Freiburg University, Freiburg, Germany, [3]Department of Geology and Centre of Hydrogeology, University of Malaga (CEHIUMA), Malaga, Spain

Key Points:
- A new approach for spatiotemporal recharge estimation for karst aquifers
- Impacts of hydroclimatic extremes on the entire karst system are elaborated
- Recharge rates are more sensitive to a precipitation decrease than an increase

Supporting Information:
- Readme
- Supplement to the analysis

Correspondence to:
A. Hartmann,
aj.hartmann@bristol.ac.uk

Citation:
Hartmann, A., M. Mudarra, B. Andreo, A. Marín, T. Wagener, and J. Lange (2014), Modeling spatiotemporal impacts of hydroclimatic extremes on groundwater recharge at a Mediterranean karst aquifer, *Water Resour. Res.*, *50*, 6507–6521, doi:10.1002/2014WR015685.

Received 7 APR 2014
Accepted 15 JUL 2014
Accepted article online 17 JUL 2014
Published online 13 AUG 2014

Abstract Karst aquifers provide large parts of the water supply for Mediterranean countries, though climate change is expected to have a significant negative impact on water availability. Recharge is therefore a key variable that has to be known for sustainable groundwater use. In this study, we present a new approach that combines two independent methods for karst recharge estimation. The first method derives spatially distributed information of mean annual recharge patterns through GIS analysis. The second is a process-based karst model that provides spatially lumped but temporally distributed information about recharge. By combining both methods, we add a spatial reference to the lumped simulations of the process-based model. In this way, we are able to provide spatiotemporal information of recharge and subsurface flow dynamics also during varying hydroclimatic conditions. We find that there is a nonlinear relationship between precipitation and recharge rates resulting in strong decreases of recharge following even moderate decreases of precipitation. This is primarily due to almost constant actual evapotranspiration amounts despite varying hydroclimatic conditions. During the driest year in the record, almost the entire precipitation was consumed as actual evapotranspiration and only little diffuse recharge took place at the high altitudes of our study site. During wettest year, recharge constituted a much larger fraction of precipitation and occurred at the entire study site. Our new method and our findings are significant for decision makers in similar regions that want to prepare for possible changes of hydroclimatic conditions in the future.

1. Introduction

Even though a large part of the water supply of Mediterranean countries is provided by karst aquifers [e.g., *Andreo et al*., 2008b; *COST*, 1995], there is limited knowledge about their sensitivity to climatic change. Climate simulations suggest that in the next 90 years Mediterranean regions will be exposed to higher temperatures and lower precipitation [*Christensen et al*., 2007]. In addition, an increase of hydroclimatic extremes can be expected in the Mediterranean, both in terms of hydrological droughts [*Milly et al*., 2005] and floods [*Hirabayashi et al*., 2013]. The impacts of these changes on karst water resources are difficult to assess [*Hartmann et al*., 2014].

For sustainable water use, groundwater recharge is the most important variable. It is the key to assess the maximum volume of water that can be used for water supply without over-exploiting the aquifer [*Seiler and Gat*, 2007]. Measured time series of groundwater levels were often used to quantify recharge over time [*Scanlon et al*., 2002], but the heterogeneity of karstified rock [*Bakalowicz*, 2005] makes this method unreliable for karst regions. The water balance method [*Carter and Driscoll*, 2006; *Jocson et al*., 2002; *Sheffer et al*., 2011] or tracer techniques [*Aquilina et al*., 2005; *Lange et al*., 2010; *Plummer et al*., 1998] were found to be more reliable to determine groundwater recharge for the time period when observations were taken. Using environmental tracers (e.g., chloride, CFCs the $^3H/^3He$ ratio, etc.) information about past recharge in karst regions can be gathered [*Dunkle et al*., 1993; *Wood and Sanford*, 1995]. GIS-based methods that use spatial information about geology, soil types, vegetation, mean annual precipitation, etc., are often used to derive time-averaged spatial distribution of karst recharge [*Allocca et al*., 2014; *Andreo et al*., 2008b; *Radulovic et al*., 2011]. All these methods may provide information about present or past recharge but for assessing future water resources availability their application is critical because they do not take into account changing boundary conditions, for instance, due to changes of climate or land use [*Hartmann et al*., 2012].

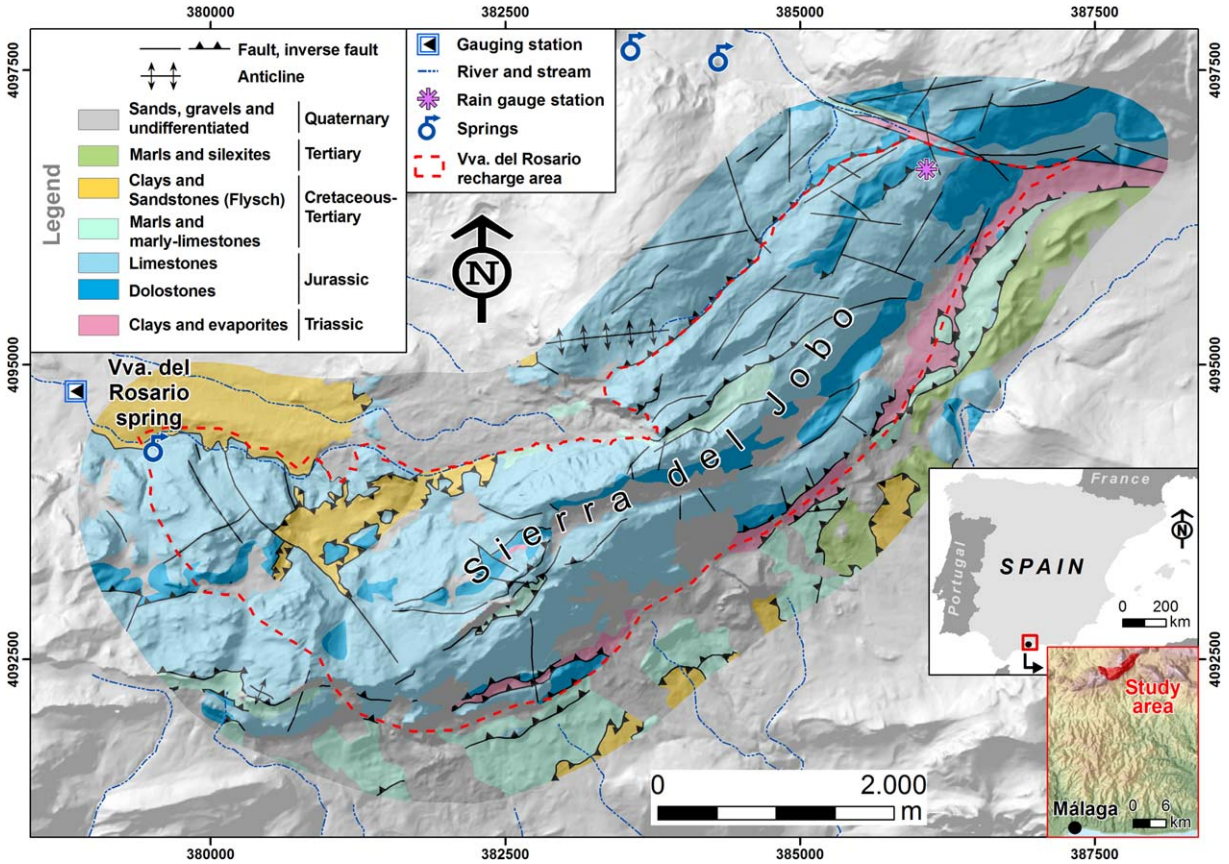

Figure 1. Map of the study site and its location in Southern Spain.

Numerical simulation models may provide better temporal information about future recharge rates. Preceding studies showed that for reliable simulations karst processes have to be considered in the model structures [*Andreu et al*., 2011; *Ireson and Butler*, 2013]. Theoretically, they are capable to simulate the spatial and temporal distribution of flow processes within a karst system including recharge. However, a lack of information about the spatial variability of karst system properties often prohibited the use of spatially distributed models [*Le Moine et al*., 2008] and only permitted the application of lumped approaches [*Jukic and Denic-Jukic*, 2009; *Rimmer and Salingar*, 2006] that provide a single time series of recharge rates without any spatial information.

In this study, we use the spatially averaged information obtained by a GIS-based recharge estimation method and combine it with the temporal information about recharge dynamics provided by a lumped process-based karst simulation model. We compare spatial distributions of recharge rates provided by the GIS-based method with those of the calibrated simulation model and translate the static GIS information into time-dependent recharge maps. We then use these maps combination to assess the sensitivity of recharge and its spatial distribution to hydroclimatic extremes; in our case an extremely wet and an extremely dry year from historical records. We finally develop 3-D conceptual models about the system functioning under average, extremely wet, and extremely dry conditions.

2. Study Area

The study area, the Villanueva del Rosario karst system, is located approximately 30 km north of the city of Malaga, Southern Spain (Figure 1). The terrain in this area is rugged, with altitudes ranging from 600 to 1640 m ASL. Prevailing climate is temperate Mediterranean, with a marked seasonal pattern in the annual distribution of precipitation. Rainfall mainly occurs in autumn, winter and, to a lesser extent, in spring time, associated with wet winds coming from the Atlantic Ocean. Mean annual precipitation recorded in the study area during the historic period (1968/1969–2009/2010) was 760 mm [*Mudarra*, 2012]. An air

temperature record for the northwest boundary of the system (over 700 m ASL) shows a mean annual temperature of close to 14°C [*Mudarra*, 2012]. From a geological standpoint, the study site consists of 400–450 m thick Jurassic dolostones and limestones (Figure 1), which are enveloped by Upper Triassic clays and evaporite rocks (mainly gypsum) at the bottom, and by Lower Cretaceous-Paleogene marly limestones and marls on the top [*Martín-Algarra*, 1987; *Peyre*, 1974]. The geological structure is formed by ENE-WSW lying folds, from which overthrusts have developed with vergence toward S-SE (Figure 1). The system is surrounded by outcrops of Flysch-type clays and sandstones. The entire structure has been affected by more recent fractures, in a mainly NW-SE direction.

In hydrogeological terms, the Villanueva del Rosario system has an approximate recharge area of 13.85 km^2 and is composed of fractured and karstified Jurassic carbonate rocks. The karst system is limited at almost all its borders by low permeability materials (Triassic and Flysch clays and Cretaceous-Paleogene marls). The only exception is the southwest border, corresponding to an open limit and delineated by geological and hydrogeological characterization of the system and by dye tracer tests [*Mudarra et al*., 2014]. Recharge occurs by direct infiltration of precipitation, while discharge occurs mainly through Villanueva del Rosario spring (260 L/s annual mean discharge rate) situated at 770 m ASL, at the northern border of the carbonate outcrops (Figure 1). The Villanueva del Rosario karst system is of great importance, as it constitutes the main source of drinking water for an urbanized area nearby. Additional background information about the hydrogeological characteristics of Villanueva del Rosario system has been described in previous works [*Mudarra and Andreo*, 2011; *Mudarra et al*., 2014]. Karst features have developed mainly on Jurassic limestones, with large karrenfields, dolines, and uvalas. There are also swallow holes, which become active during large storm events. Epikarst features are formed within bare carbonate rock. A patchy soil cover exists up to 10–15 cm thick, and located especially in karst depressions and where slopes are low. There, only scant vegetation of the Mediterranean type can be found. Except for some slight farming activities, the study area is influenced by human activities [*Mudarra and Andreo*, 2011].

3. Methodology

3.1. Spatial Distribution of Recharge (Averaged Over Time)

We used the APLIS method [*Andreo et al*., 2008b] to estimate the average spatial distribution of recharge is. APLIS estimates the mean annual recharge of carbonate aquifers, expressed as a percentage of precipitation. Input parameters are average annual precipitation, its spatial distribution, and a combination of the physical variables that have found to be most influential [*Durán et al*., 2004]: altitude (*A*), slope (*P*), lithology (*L*), infiltration landforms (*I*), and soil type (*S*). To obtain a map of the average recharge rate, available information about *A*, *P*, *L*, *I*, and *S* is transformed by a ranking system into dimensionless values from 1 to 10 [*Andreo et al*., 2008b] and combined by:

$$\overline{R_j} = \frac{A_j + P_j + 3L_j + 2I_j + S_j}{0.9} \cdot F_{h,j} \quad (1)$$

where $\overline{R}_i$ is the mean annual recharge rate at a location *j*, and $F_{h,j}$ acts as a correction factor between 0.1 and 1 depending on the permeability of the aquifer [*Marín*, 2009]. A summary of the APLIS input variables and their description are provided in Table 1. The APLIS method was successfully applied to eight carbonate aquifers in Southern Spain, representative of a wide range of climatic and geologic [*Andreo et al*., 2008b] and worldwide [*Farfán et al*., 2010; *Gerner et al*., 2012; *Zagana et al*., 2011].

3.2. Temporal Distribution of Recharge (Avergaged Over Space)

3.2.1. Model Structure

The process-based VarKarst model is used to assess the temporal evolution of recharge (Figure 2). The model was previously developed for another karst system in Southern Spain [*Hartmann et al*., 2013a] and it was already applied to various settings in the Mediterranean, Middle Europe, and the Middle East [*Hartmann et al*., 2013b]. Similar to the Probability Distributed Model (PDM) [*Moore*, 2007] or the variable karst recharge model [*Hartmann et al*., 2012], VarKarst includes the spatial variability of (i) soil and epikarst depths, (ii) fractions of concentrated and diffuse recharge to the groundwater, (iii) epikarst hydrodynamics, and (iv) groundwater hydrodynamics using the Pareto functions that are applied to a set of *N* model compartments (Figure 2). A detailed description of the model is provided in the supporting information and a list of the model parameters is provided in Table 1.

Table 1. List of APLIS Input Variables and Description

Input Parameters	Description	Rank Values	Source
A	Altitude	1 (low), . . .,10 (high)	DEM; MDT05/MDT05-LIDAR, Centro Nacional de Información Geográfica, Instituto Geográfico Nacional, Ministerio de Fomento, Gobierno de España
P	Slope	1 (high), . . .,10 (low)	
L	Lithodology	1 (low permeability rock), . . .,10 (high permeability rock)	National geological map; serie MAGNA, scale 1:50,000, Spanish Geological Survey
I	Infiltration landforms	1 (not abundant), . . .,10 (many dolines sinkholes, etc.)	Field survey [*Mudarra*, 2012]
S	Soil	1 (vertisols), . . .,10 (leptosols)	Regional soil maps; project LUCDEME "Proyecto de Lucha contra la Desertificación en el Mediterráneo," scale 1:100,000
F_h	Aquifer storage capacity	0.1 (low), . . .,1 (high)	National geological map; serie MAGNA, scale 1:50,000, Spanish Geological Survey

3.2.2. Model Calibration and Evaluation

Preceding studies showed that hydrochemical data can be useful for the calibration and evaluation of hydrological models for karst systems [*Hartmann et al*., 2013a, 2012]. Here we assess the usefulness of hydrochemical data by comparing the results of a first model calibration by discharge with a second calibration using both discharge and hydrochemical information (Cl, NO_3, and SO_4). We use a modified version of the Kling-Gupta efficiency *KGE* [*Gupta et al*., 2009] as measure of efficiency, which is defined by

$$KGE = 1 - \sqrt{(r-1)^2 + (\alpha-1)^2 + (\beta-1)^2} \tag{2}$$

$$\text{with } \alpha = \frac{\sigma_S}{\sigma_O} \text{ and } \beta = \frac{\mu_S}{\mu_O} \tag{3}$$

Hereby, r is the linear correlation coefficient between simulations and observations, μ_s/μ_o and σ_s/σ_o are the mean and standard deviation of simulations and observations, respectively. α represents the variability; β stands for the bias. The recharge area of our studied system, which mainly controls the water balance of the karst system [*Hartmann et al*., 2013b], is already known (13.85 km^2, see section 2) and *KGE* can be simplified as follows (likewise to *Hartmann et al*. [2013a]):

$$KGE_Q = 1 - \sqrt{(r-1)^2 + (\alpha'-1)^2} \tag{4}$$

In order to exclude water balance completely, the standard deviations in α are normalized by the means of simulated and observed discharges:

$$\alpha' = \frac{\sigma_S/\mu_S}{\sigma_O/\mu_O} \tag{5}$$

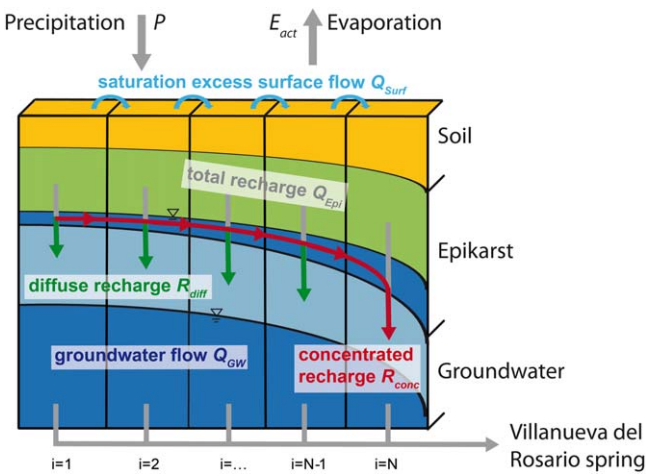

Figure 2. Structure of the VarKarst Model (*Hartmann et al*. [2013a], modified).

An analog procedure is applied for hydrochemistry to ignore effects of contamination due to slight farming activities in the region [*Mudarra and Andreo*, 2011]. *Hartmann et al*. [2013a] showed that for hydrochemistry the standard deviations in α have not to be normalized:

$$KGE_Q = 1 - \sqrt{(r-1)^2 + (\alpha'-1)^2} \tag{6}$$

Table 2. VarKarst Model Parameters, Descriptions, and Ranges for Calibration and Uncertainty Analysis

			Parameter Ranges		Data Used for Calibration	
Parameter	Description	Unit	Lower	Upper	Q	Q, Cl, NO_3, SO_4
$V_{mean,S}$	Mean soil storage capacity	mm	0	500	394.7	207.9
$V_{mean,E}$	Mean epikarst storage capacity	mm	0	500	498.4	387
a_{SE}	Soil/epikarst depth variability constant		0	2	1.77	0.35
$K_{mean,E}$	Epikarst mean storage coefficient	day^{-1}	1	50	1	1.06
a_{fsep}	Recharge separation variability constant		0	2	1.84	1.14
K_C	Conduit storage coefficient	day^{-1}	1	20	6.1	8.2
a_{GW}	Groundwater variability constant		0	2	1.57	2
$log\ Geo_{Cl}$	Equilibrium concentration of Cl in matrix	mg L^{-1}	0	5	4.8	0.8
$logGeo_{SO4}$	Equilibrium concentration of SO4 in matrix	mg L^{-1}	0	5	1.6	1.6
a_{Geo}	Equilibrium concentration variability constant		0	2	1.87	0.67
KGE_{all}	Performance concerning all data used for calibration		0	1	0.91	0.7
KGE_Q	Performance concerning discharge		0	1	0.91	0.89
$KGE_{C,Cl}$	Performance concerning Cl		0	1		0.7
$KGE_{C,NO3}$	Performance concerning NO_3		0	1		0.45
$KGE_{C,SO4}$	Performance concerning SO_4		0	1		0.75

$$\alpha = \frac{\sigma_S}{\sigma_O} \tag{7}$$

A 3 year record (hydrological years 2006/2007–2008/2009) spring discharge Cl, NO_3, and SO_4 concentrations (of precipitation and discharge) was available for calibration. Model parameters are found by the Shuffled Complex Evolution Metropolis algorithm SCEM [*Vrugt et al.*, 2003]. During the first calibration (discharge only) KGE_Q is used as objective function. During the second calibration (discharge and hydrochemistry), equal weights for KGE_Q and KGE_C are applied (1/4 each). To obtain reasonable initial conditions, we perform a 3 year spin-up.

3.3. Evaluation of the Recharge Estimation Methods

A split sample test [*Klemeš*, 1986] with discharge observations beyond the calibration period is performed (hydrological years 1991/1992–1998/1999) to evaluate the prediction capabilities of VarKarst. This period also evaluates the model performance for the two extreme years that are analyzed later (section 3.5). For the evaluation of annual recharge rates given by APLIS and VarKarst, we look at the differences of their recharge rates for the entire calibration period (2006/2007–2008/2009), and its first (2006/2007) and last year (2008/2009) that had less and more precipitation than the average (Table 2).

An agreement of recharge rates obtained by the independent methods will provide some indication for a realistic values taking into account that both methods were developed and evaluated for the Southern Spanish karst environment before. However, there is still some probability that both methods are wrong at this particular site. To avoid that, we evaluate both methods with 3 years of observed recharge rates. They are obtained by dividing mean annual observed discharge during the calibration period [transformed into (mm/a) using the recharge area, section 2] by annual observed precipitation (mm/a). Comparing both methods with real recharge rates for individual years and the entire 3 year period will provide stronger indication for their performance than their intercomparison.

3.4. Combination of Spatial and Temporal Recharge Distributions

During the 3 years of the calibration period, around 750 mm/a of precipitation was measured, which almost represent the long-term annual average of 770 mm/a. This similarity can be used to combine the spatial

average distribution of recharge obtained by APLIS with the temporal distribution of recharge obtained by the VarKarst model. Using frequency distributions of the APLIS average recharge rates and of the mean recharge rates of the N VarKarst model compartments, the VarKarst model compartments can spatially be attributed the APLIS raster cells:

$$i \xrightarrow{\text{spatial attribution}} j(R) \quad \forall \quad j(R) : r_{i-1} < R \leq r_i, i = 1 \ldots N \tag{8}$$

i.e., VarKarst model compartment i is attributed to all APLIS raster cells $j(R)$ with the recharge rate R that is between the recharge rates r_{i-1} and r_i of the VarKarst model compartments $i-1$ and i. For example, if model compartment $i = 25$ provides recharge rates of 35%–40%, then it represents all APLIS raster cells that fall in the same range of recharge rates $j(R)$: $35\% < R \leq 40\%$. Since each of these raster cells have a spatial reference, model compartment $i = 25$ can be attributed to all their locations. By the same procedure (equation (8)), each of the N model compartments can be attributed to a set of APLIS raster cells that all together cover the entire study area (Figure 5) and a spatial reference to the temporally dynamic simulations of the VarKarst model can be provided.

To evaluate the value of hydrochemical data this procedure is performed twice, once with the parameter set obtained by calibrating the VarKarst model with discharge only, and a second time by calibrating with discharge and hydrochemical data. Having attributed each VarKarst model compartment to a set of APLIS raster cells, recharge maps for the whole calibration period and for individual years can be obtained.

3.5. Spatiotemporal Sensitivity of Recharge on Hydroclimatic Extremes

The validation time series contains one of the wettest (1995/1996, 1560 mm) and one of the driest (1998/1999, 275 mm) hydrological years recorded in the region since the 1950s. For these years, maps of recharge rates are produced by calculating the annual recharges of each of the N VarKarst model compartments and attributing them to their locations within the study site. For comparison, we also create a map of recharge rates during average conditions (2006/2007–2008/2009, 750 mm of mean annual precipitation).

Each model compartment provides simulations of all water balance components (precipitation, actual evapotranspiration, diffuse recharge, concentrated recharge, groundwater flow, and spring discharge). Using them and the spatial attribution procedure, allows us to develop a conceptual models of the hydrological behavior of the karst system during the selected years that can be used as tool of communication for decision makers and water management.

4. Results

4.1. Individual Estimation of Spatial and Temporal Distribution of Recharge

By APLIS (equation (1)), mean annual average recharge rates between 20% and 80% were found in the study area (Figure 3a). The lowest recharge rates occurred in Tertiary, Cretaceous-Tertiary, and Triassic areas (Figure 1), while Quaternary regions showed moderate recharge rates. Medium to high recharge rates were found in Jurassic areas increasing with higher altitude. During the 3 years of calibration, the VarKarst model showed daily recharge rates ranging from 0% up to 100% depending on the varying hydroclimatic conditions over time (Figure 3b). Mostly after longer dry periods, the first rainfall event created no or just little recharge. After longer wet periods, very high recharge rates were simulated. The strong seasonality of rainfall reflects itself in a strong seasonality of recharge. On average, APLIS and the VarKarst model produced recharge rates of 46.6% and 51.5%, respectively (Table 2).

4.2. Evaluation of the Recharge Estimation Methods

With and without using hydrochemical information, calibration of VarKarst reaches high performance concerning spring discharge (Figure 4 and Table 1, $KGE_Q = 0.89$–0.91). However, when hydrochemistry is added to the calibration, optimized parameter values change (Table 1) and a multiobjective fit for discharge ($KGE_Q = 0.89$) and hydrochemistry ($KGE_{C,CL} = 0.70$, $KGE_{C,NO3} = 0.45$, and $KGE_{C,SO4} = 0.75$) was achieved. During the validation period, this is also supported by a superior KGE_Q of 0.74 using the parameter set that includes hydrochemistry, compared to the parameter set whose calibration only considered discharge ($KGE_Q = 0.65$). Both APLIS and the VarKarst model slightly under-estimate observed recharge (Table 2) but deviations were $<10\%$. However, considering individual years, VarKarst model clearly outperforms the

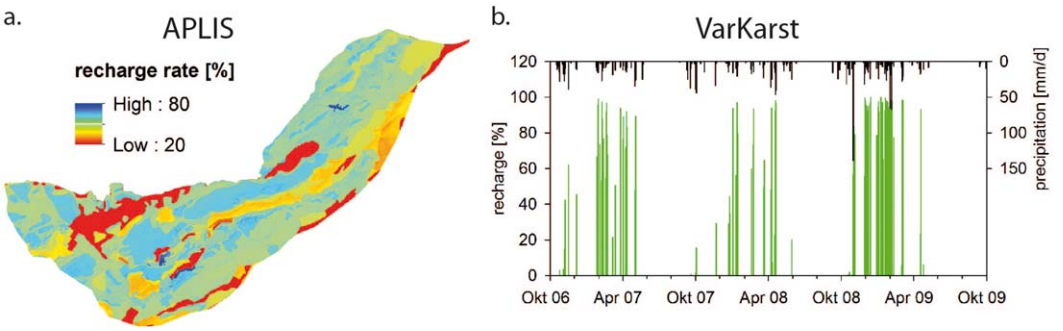

Figure 3. (a) Average spatial distribution of recharge obtained by APLIS and (b) lumped annual time series obtained by the VarKarst model (averaged over the 50 model compartments for each time step).

APLIS, because the latter cannot reflect changes of recharge conditions during years that deviate from average conditions.

4.3. Combination of Spatial and Temporal Distribution of Recharge

There is acceptable agreement between recharge rate frequencies by APLIS and by the $N = 50$ VarKarst model compartments for probabilities >0.3 in their recharge frequency distribution (Figure 5a) provided that VarKarst calibration used discharge and hydrochemistry. Below probabilities of 0.3, APLIS shows lower recharge rates than the VarKarst model. The areas of deviation represent $\sim$4.15 km^2 of the whole recharge area (13.85 km^2). Using only discharge for calibration, there was only little agreement between the two methods, which was another indicator for the reliability of simulations obtained by the VarKarst calibration including both discharge and hydrochemistry.

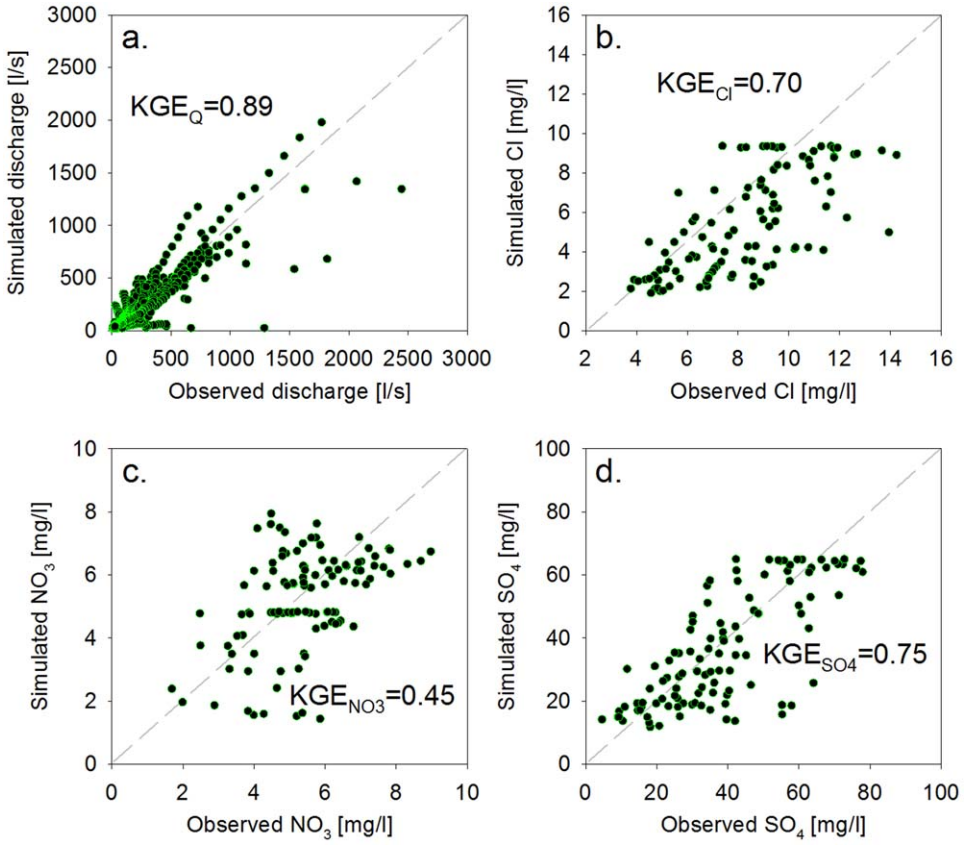

Figure 4. Observed versus simulated (a) Cl, (b) NO_3, (c) SO_4, and (d) discharge obtained by calibration of the VarKarst model using equally weighted discharge, Cl, NO_3, and SO_4 observations.

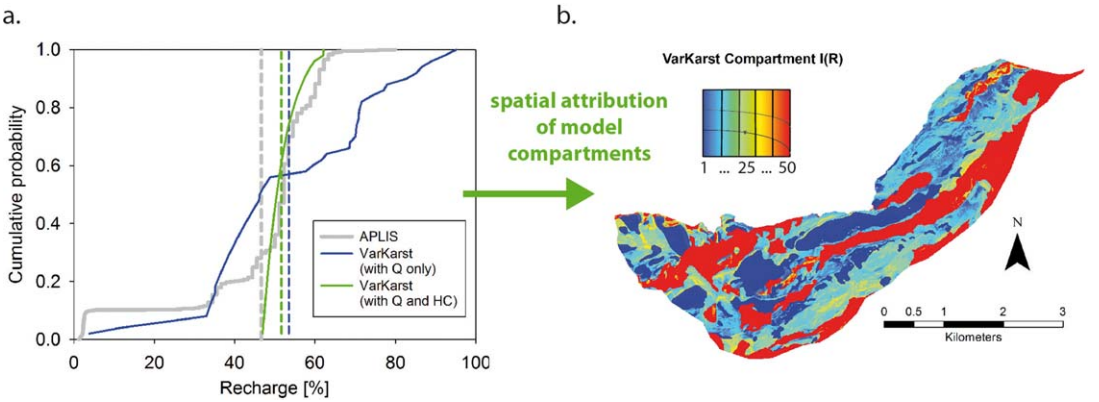

Figure 5. (a) spatial distributions of recharge obtained from APLIS, the VarKarst model calibrated with discharge only (blue), and the model calibrated by discharge and all solutes (green) and (b) the result of the new spatial distribution procedure; mean recharge rates over the whole area indicated by dashed lines in the respective color.

Using equation (24), each VarKarst model compartment was provided a spatial reference using the APLIS raster cells with corresponding recharge rates. Figure 5b shows that there is a nonuniform abundance of attributed model compartments over the study area. All regions with low to moderate recharge rates (Tertiary, Cretaceous-Tertiary, Quaternary, and Triassic areas, Figure 1) were attributed to the VarKarst model compartments with greater soil and epikarst thickness ($i \approx 45$–50). These were mostly the regions with deviations between APLIS and VarKarst (probabilities ≤ 0.3 in the recharge frequency distribution, Figure 5a). Areas attributed to model compartments $i \approx 1$–20 corresponded to the limestone and dolostone areas with decreasing soil and epikarst depths and increasing altitude (Jurassic, Figure 1). Only few locations are attributed to compartments $i \approx 21$–44.

4.4. Spatiotemporal Sensitivity of Recharge on Hydroclimatic Extremes

During the average period (2006/2007–2008/2009), a slightly larger part of the recharge entered in diffuse form at the model compartments with lower soil and epikarst depths ($i < 28$, Figures 6a, 6d, and 6g). Evapotranspiration increased at areas with greater soil and epikarst depth. A significant fraction of the spring discharge was provided by low permeability groundwater compartments (matrix, $i < N$). Unlike diffuse recharge, the contributions of the matrix reach their maximum at around $i = 6$. In accordance to the fraction of concentrated recharge, slightly less than half of the spring discharge was provided by preferential flow through the high-permeability domains (conduits, $i = N$).

In the extremely wet year (1995/1996), diffuse as well as concentrated recharge increased significantly at all model compartments (Figures 6b, 6e, and 6h). The contribution of diffuse recharge from model compartments with low soil and epikarst depths ($i = 1, \ldots, 28$) remained larger than the contribution of concentrated recharge from compartments with increasing depths. Compared to the average year the amount of evapotranspiration almost stayed the same. The peak of matrix discharge moved to $i = 12$ and a minimum occurred very close to $i = 1$. Concentrated groundwater discharge ($i = N$) strongly increased. In the extremely dry year (1998/1999), a drastic reduction of recharge could be observed (Figures 6c, 6f, and 6i): Only at the low soil and epikarst compartments ($i \leq 16$) small recharge occurred while in remaining model compartments almost all precipitation was consumed by evapotranspiration. Groundwater discharge from the matrix exceeded the dry year's recharge. Since there was almost no recharge in the compartments with $i > 16$, only insignificant amounts of concentrated discharge ($i = N$) occurred.

5. Discussion

5.1. Spatial and Temporal Distribution of Recharge

The spatially averaged recharge rate found by the APLIS method (46.6%) is in agreement with other studies in the region that found recharge rates from 32% to 54% [*Andreo et al.*, 2008b]. Areas of low recharge correspond to nonlimestone and nondolostone areas in the lower altitudes (clays, sandstones, marls). Areas of high recharge are represented by the limestone and dolostone regions. Within these areas recharge

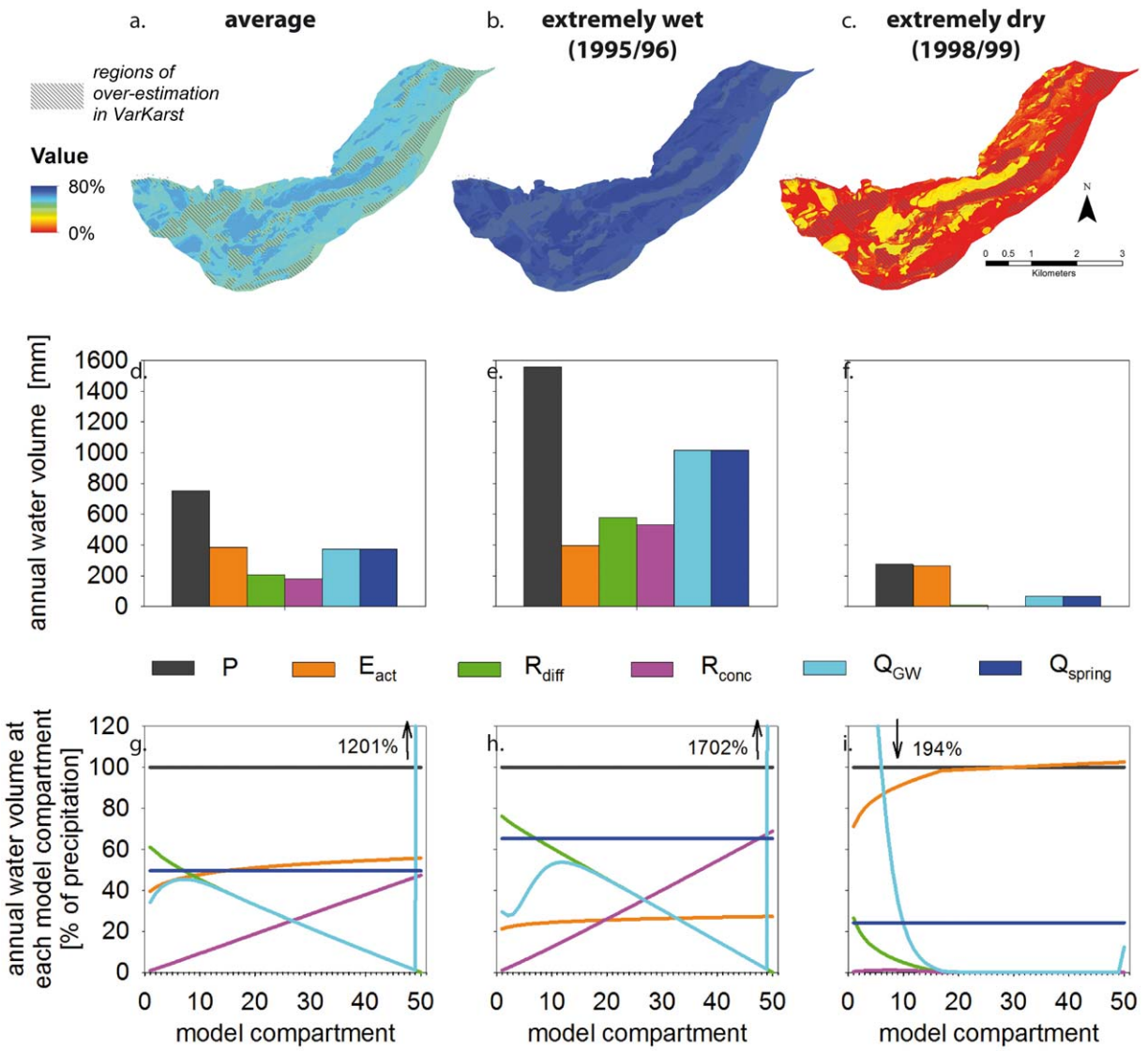

Figure 6. Spatial distribution of recharge (a–c) over the whole recharge area, (d–f) spatial average of all water balance components, (g–i) their evolution among the individual model compartments under (Figures 6a, 6d, and 6g) average conditions, (Figures 6b, 6e, and 6h) under extremely wet conditions, and (Figures 6c, 6f, and 6i) under extremely dry conditions (P: precipitation, I: infiltration, E_{act}: actual evapotranspiration, R_{diff}: diffuse recharge, R_{conc}: concentrated recharge, Q_{GW}: groundwater discharge from the individual model compartments, Q_{spring}: spring discharge).

increases with altitude. Such relation is realistic since the higher regions have lower soil thickness and different vegetation. Hence, less water is lost to evapotranspiration. In another study, *Heilman et al*. [2014] obtained similar results by comparing woodland and grassland evaporation at a karst region. Exceptions are locations of preferential infiltration (sinkholes) that show higher recharge rates in moderate altitudes. Such controls on recharge were also found in other studies in the Mediterranean [*Allocca et al*., 2014]. With an average recharge rate of 51.5%, the VarKarst model results are also in the same realistic range as the APLIS method. The simulated temporal evolution of recharge rates reflects the variability of rainfall events and their seasonality. Depending on the preceding soil moisture conditions, time series of simulated recharge rates reach up to 100%, which is in accordance to other recharge simulation studies [*Hartmann et al*., 2013a; *Ireson and Butler*, 2013].

5.2. Reliability of the Two Recharge Estimation Methods and Their Combination

In general, the VarKarst model shows poorer performance for its hydrochemical simulations than for its discharge simulations (Figure 4). This may partly be attributed to the simple representation of transport

Table 3. Water Balance Components of the VarKarst Model for Average Conditions and the Extreme Hydroclimatic Years Compared to the APLIS Recharge Rates[a]

	VarKarst						APLIS	Observed	
Year	P (mm)	E_{act} (mm)	R_{diff} (mm)	R_{conc} (mm)	Q_{spring} (mm)	R (%)	R (%)	Q_{spring} (mm)	R^b (%)
2006/2007–2008/2009 (average)	752.3	384.3	206.9	180.8	372.7	51.5	46.6	391	52
2008/2009 (wet)	932.3	330.6	341	306.2	612.1	69.4	46.6	692.3	74.3
2006/2009 (dry)	642.4	390.8	135.8	114.6	246.9	39	46.6	173.5	27

[a]P: Precipitation, E_{act}: Actual Evapotranspiration, R_{diff}: Diffuse Recharge, R_{conc}: Concentrated Recharge, Q_{spring}: Spring Discharge, R: Total Recharge

[b]Estimated by ratio of observed precipitation (mm) and Q (mm) for the respective year.

processes within the model but it may also be due anthropogenic impacts on water quality that are not included in the model or calibration procedure. However, considering (1) the overall acceptable multiobjective agreement for discharge and hydrochemical observations at the spring, and (2) the moderate decrease of simulation performance during the validation period that also include the extremely wet and dry years, we can state that the VarKarst model provides an acceptable performance when both discharge and hydrochemical observations are used for calibration. The same was found when VarKarst was applied to another karst system nearby [*Hartmann et al*., 2013a]. Compared to this study, the present calibration by discharge and hydrochemical observations yielded similar parameter values.

APLIS and VarKarst independently provided similar mean recharge rates and distributions (Table 3), which indicates that either of the two-independent methods provided realistic results. The agreement of mean annual recharge rates found by the comparison with observed spring discharges further corroborates that both methods perform satisfactory. Since both methods were developed for the same region in Southern Spain this is no big surprise. But it has to be kept in mind that the lack of spatial observations of recharge rates within the system prohibits an evaluation of the spatial performance of APLIS and its combination with the VarKarst model.

Considering the spatial distribution of recharge (Figure 5), both methods agree for probabilities >0.3, but only when discharge and hydrochemistry were used to calibrate the VarKarst model. This further corroborates that the multiobjective calibration of VarKarst was superior to a calibration that considered discharge only. The probabilities of ≤ 0.3 correspond to recharge rates $\leq 45\%$ which largely constituted mostly the non-Jurassic areas of the study site. Since the VarKarst model was developed for karstified carbonate rock regions [*Hartmann et al*., 2013a] and APLIS is also capable of considering different types of lithology [*Andreo et al*., 2008b] one may assume that APLIS provides the more reliable recharge estimates for low recharge areas.

Despite the deficiencies mentioned above, the VarKarst model provides better agreement with observed recharge rates than APLIS during individual years (Table 2). During the last year of the calibration period (2008/2009, 932 mm of precipitation), VarKarst simulates that a 24% increase of precipitation resulted in a 35% increase of recharge rate (compared to the average period). For the first year (2006/2007, 642 mm of precipitation), a 14% decrease of precipitation resulted in a 24% decrease of recharge. The superiority of the VarKarst model is due to its process-based structure that allows for a nonlinear relationship between precipitation and recharge rates that was also found in other studies [*Gunkel and Lange*, 2011; *Martínez-Santos and Andreu*, 2010]. When annual precipitation and recharge rates during calibration and validation periods are plotted together (Figure 7), a logarithmic relationship suggests that in years with precipitation below 250 mm/a recharge completely declines. This almost happened in the extremely dry year in 1998/1999. Plotting annual rainfall against recharge volumes, *Samuels et al*. [2009] found a linear relationship at recharge area of the springs feeding the Upper Jordan River, Israel. Transforming their recharge volumes into recharge rates will show a logarithmic relation as in this study. In their case, recharge rates will reach 0% after rainfall falling below 400 mm/a. The increasing slope low annual precipitation indicates that recharge rates at our study site are more sensitive to a decrease than an increase of precipitation. Hence, the expected future decrease of precipitation over the Mediterranean [*Hartmann et al*., 2014; *IPCC*, 2007] will have an amplified negative impact on water supply at the study area. Using historic data for this assessment implies that rainfall frequencies will remain the same. If the general characteristics of rainfall change,

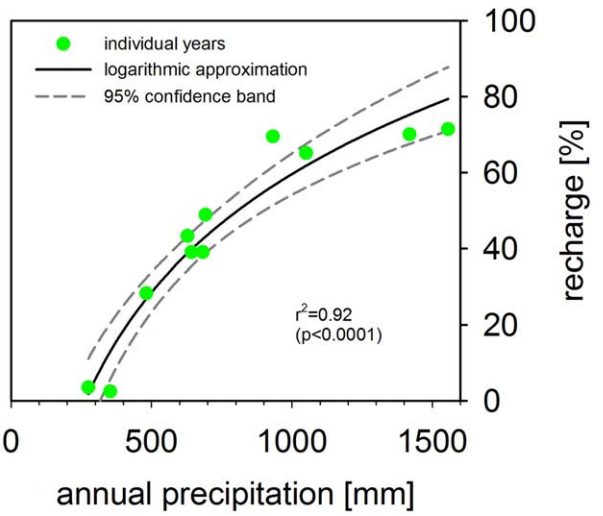

Figure 7. Relation between annual precipitation and recharge rate simulated by the VarKarst model for calibration and validation period.

the shape of the logarithmic relationship in (Figure 7) may change. However, in a similar study [*Samuels et al*., 2010] showed that changes in the form of precipitation are nearly insignificant in terms of changing discharge characteristics.

5.3. Shifting System Dynamics Under Extreme Hydroclimatic Conditions

APLIS and VarKarst could be combined in at least ~70% of the study area (Figure 5). This combination could be used to understand the karst system's quantitative recharge and subsurface flow characteristics (Figure 6) and to establish conceptual models of the karst system dynamics under different hydroclimatic conditions (Figure 8).

During average hydroclimatic conditions (Figure 8b), a slightly larger part of the recharge enters as diffuse recharge at higher-altitude Jurassic areas with lower soil and epikarst depths. Slightly less than half of the simulated recharge occurs in concentrated form, predominantly at medium to lower altitude areas with high subsurface permeability. Evapotranspiration increases toward areas with thicker soils at low altitudes and in Tertiary, Cretaceous-Tertiary, Quaternary, and Triassic areas. A significant fraction of the spring discharge is provided by low permeability groundwater compartments (matrix of the karst aquifer). Slightly less than half of the spring discharge is provided by preferential flow through high-permeability domains (conduits), with increasing fractions toward the spring outlet (compartment $i = N$). These average conditions represent the behavior of a well karstified system as found in other studies [*Fleury et al*., 2009; *Schmidt et al*., 2014].

Compared to the average year the amount of evapotranspiration remains almost the same for the extremely wet (Figure 8c) and the extremely dry years (Figure 8d). Diffuse as well as concentrated recharge increase significantly over the entire study area in the wet year, while in the extremely dry year a drastic reduction of recharge can be observed that only shows marginal recharge at the high-latitude Jurassic areas. Concentrated flow in the high-permeability domains (conduits) strongly increases in the extremely wet year. During the extremely dry year the spring is mainly fed by water from the low permeability domains (matrix).

Hence, if climate shifted toward wetter conditions, the stronger contribution of preferential flow would provide the appearance of a more dynamic hydrological system [*El-Hakim and Bakalowicz*, 2007; *Mangin*, 1974]. And if such hydroclimatic conditions remained for a very long time, carbonate rock dissolution could be expected to increase. Hence, the dynamics of karstification would increase, too [*Ford and Williams*, 2007; *Hartmann et al*., 2014]. On the other hand, if climate shifted to dryer conditions, the system would appear like a matrix dominated karst system, as found for instance by *Butscher and Huggenberger* [2008]. However, during high-intensity events, preferential flow paths can still produce fast flow including its threats on water quality [*Andreo et al*., 2008a; *Goldscheider*, 2003].

6. Conclusions

In this study, we presented the combination of two independent methods for estimating karst recharge. One of them (APLIS) is based on spatial information and provides maps of average recharge rates. The second (VarKarst) is a process-based simulation model that considers spatial variability of karst properties by statistical distribution functions only, but provides a time series of recharge without explicit spatial

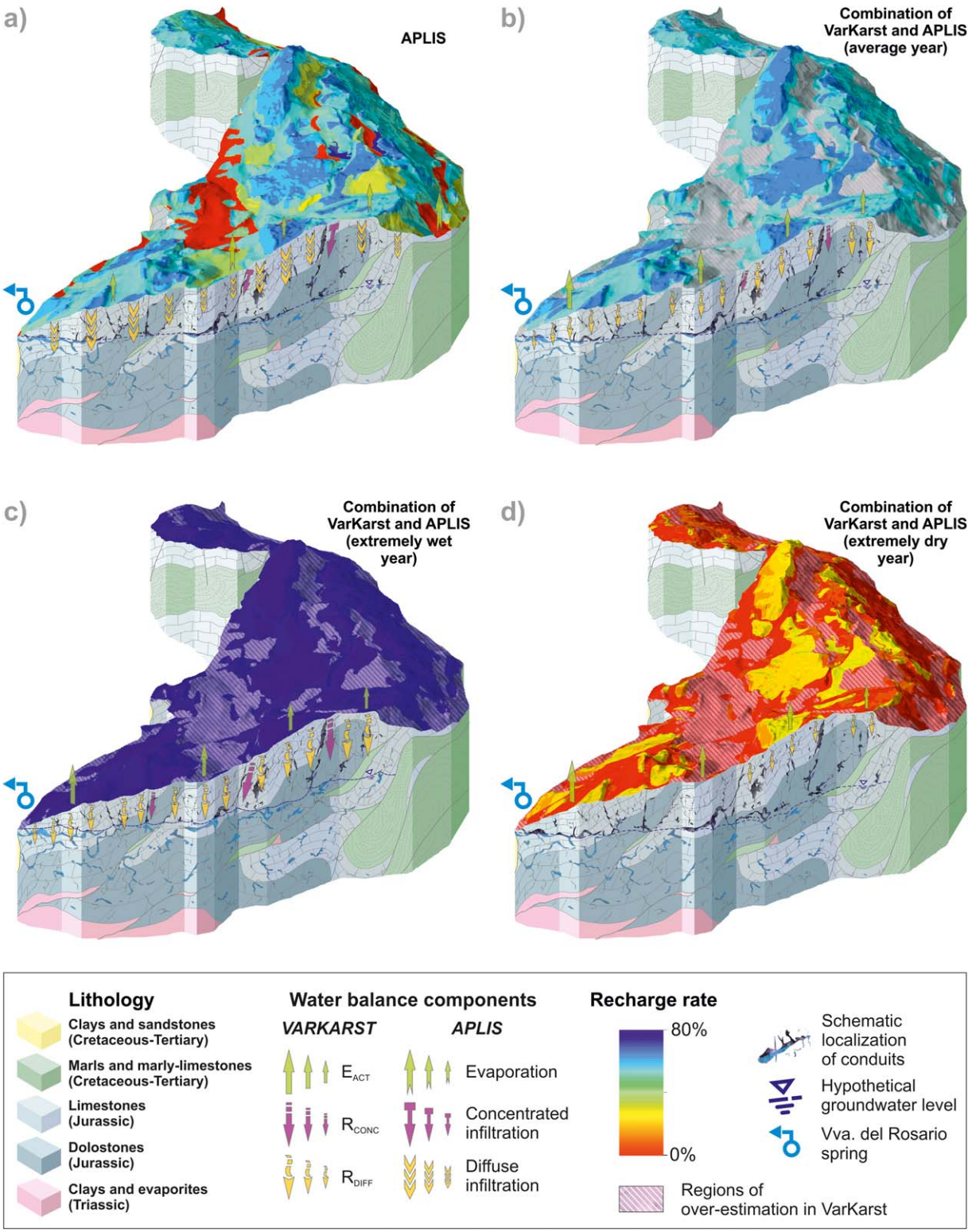

Figure 8. Conceptual model of the karst system for (b) the average period (2006/2007–2008/2009), (c) the extremely wet year (1995/1996), and (d) the extremely dry year (1998/1999) obtained by the combination of the VarKarst model and APLIS; and (a) for comparison the mean annual recharge obtained by the APLIS method alone.

information. In our study area, both methods independently provided acceptable estimates for recharge during average hydroclimatic conditions. Thus, we combine their capabilities to estimate spatiotemporal distributions of recharge and subsurface dynamics under extremely wet and extremely dry conditions. We

show that the nonlinear storage and flow dynamics result in a nonlinear relationship between precipitation and recharge rate that indicates that the recharge of our study site is more sensitive to a decrease than to an increase of precipitation. We could show that during extremes evapotranspiration almost remains the same compared to average conditions. Concentrated recharge and preferential flow through the conduits strongly increases during wet conditions, while diffuse recharge at higher altitudes of our study area and diffuse matrix flow dominate droughts. Then, the spring is fed by water from the preceding years stored in the matrix of the karst aquifer.

Our analysis provides further evidence that the calibration of process-based models with hydrochemical data can provide more realistic results than a calibration by discharge only [*Bishop et al*., 2004; *Kuczera and Mroczkowski*, 1998; *Son and Sivapalan*, 2007]. Similar to other modeling studies that deal with hydrochemical information, our hydrochemical data set had only a coarse temporal resolution compared to discharge. Spatial disaggregation of the signal at a spring or stream could even be more detailed and reveal more information about process characteristics of a hydrological system if hydrochemical data was available in higher resolution [e.g., see *Kirchner and Neal*, 2013].

Our new method transforms the originally lumped simulations of VarKarst into distributed simulations. Our combination of process-based modeling and GIS data analysis allows us to circumvent the problem of data scarcity that most distributed karst models are presently facing [*Hartmann et al*., 2014]. Moreover, we could assess the impact of hydroclimatic extremes on recharge and on entire system dynamics. We are confident that our conceptual models realistically elaborate the impact of possible changes on the recharge and on subsurface dynamics of a typical Mediterranean karst. This might help decision makers in karst regions with similar climate to adapt their water management strategies under possible future changes.

Acknowledgments
This work was supported by a fellowship within the Postdoc Programme of the German Academic Exchange Service (DAAD). Furthermore, it is a contribution of the Research Group RNM-308 of Junta de Andalucía to the projects IGP 598 of UNESCO and CGL2012-32590 of DGICYT. The data used in this study were provided by the Department of Geology and Centre of Hydrogeology of the University of Malaga (CEHIUMA), Malaga 29071, Spain.

References

Allocca, V., F. Manna, and P. De Vita (2014), Estimating annual groundwater recharge coefficient for karst aquifers of the southern Apennines (Italy), *Hydrol. Earth Syst. Sci.*, *18*(2), 803–817, doi:10.5194/hess-18-803-2014.

Andreo, B., N. Ravbar, and J. M. Vías (2008a), Source vulnerability mapping in carbonate (karst) aquifers by extension of the COP method: Application to pilot sites, *Hydrogeol. J.*, *17*(3), 749–758, doi:10.1007/s10040-008-0391-1.

Andreo, B., J. Vías, J. Durán, P. Jiménez, J. López-Geta, and F. Carrasco (2008b), Methodology for groundwater recharge assessment in carbonate aquifers: Application to pilot sites in southern Spain, *Hydrogeol. J.*, *16*(5), 911–925.

Andreu, J. M., F. J. Alcalá, Á. Vallejos, and A. Pulido-Bosch (2011), Recharge to mountainous carbonated aquifers in SE Spain: Different approaches and new challenges, *J. Arid Environ.*, *75*(12), 1262–1270, doi:10.1016/j.jaridenv.2011.01.011.

Aquilina, L., B. Ladouche, and N. Dorfliger (2005), Recharge processes in karstic systems investigated through the correlation of chemical and isotopic composition of rain and spring-waters, *Appl. Geochem.*, *20*(12), 2189–2206, doi:10.1016/j.apgeochem.2005.07.011.

Bakalowicz, M. (2005), Karst groundwater: A challenge for new resources, *Hydrogeol. J.*, *13*, 148–160.

Bishop, K., J. Seibert, S. Kohler, and H. Laudon (2004), Resolving the Double Paradox of rapidly mobilized old water with highly variable responses in runoff chemistry, *Hydrol. Processes*, *18*, 185–189.

Butscher, C., and P. Huggenberger (2008), Intrinsic vulnerability assessment in karst areas: A numerical modeling approach, *Water Resour. Res.*, *44*, W03408, doi:10.1029/2007WR006277.

Carter, J., and D. Driscoll (2006), Estimating recharge using relations between precipitation and yield in a mountainous area with large variability in precipitation, *J. Hydrol.*, *316*(1–4), 71–83, doi:10.1016/j.jhydrol.2005.04.012.

Christensen, J. H., et al. (2007), Regional climate projections, in *Climate Change 2007: The Physical Science Basis. Contribution of Working Group I to the Fourth Assessment Report of the Intergovernmental Panel on Climate Change*, edited by S. Solomon et al., pp. 996, Cambridge Univ. Press, Cambridge, U. K.

COST (1995), COST 65: Hydrogeological aspects of groundwater protection in karstic areas, Final report (COST action 65), *Rep. EUR 16547*, 446 pp., Bruessel, Belgium.

Dunkle, S. A., L. N. Plummer, E. Busenberg, P. J. Phillips, J. M. Denver, P. A. Hamilton, R. L. Michel, and T. B. Coplen (1993), Chlorofluorocarbons (CCl3F and CCl2F2) as dating tools and hydrologic tracers in shallow groundwater of the Delmarva Peninsula, Atlantic Coastal Plain, United States, *Water Resour. Res.*, *29*(12), 3837–3860, doi:10.1029/93WR02073.

Durán, J., B. Andreo, J. Vías, J. López-Geta, F. Carrasco, and P. Jiménez (2004), Classification of carbonate aquifers in the Betic Cordillera in accordance with recharge rates [in Spanish], *Boletín Geol. Minero*, *115*(2), 199–210.

El-Hakim, M., and M. Bakalowicz (2007), Significance and origin of very large regulating power of some karst aquifers in the Middle East: Implication on karst aquifer classification, *J. Hydrol.*, *333*(2–4), 329–339.

Farfán, H., J. L. Corvea, and I. de Bustamante (2010), Sensitivity analysis of APLIS method to compute spatial variability of karst aquifers recharge at the National Park of Viñales (Cuba), in *Advances in Research in Karst Media*, edited by B. Andreo et al., pp. 19–24, Springer, Berlin.

Fleury, P., B. Ladouche, Y. Conroux, H. Jourde, and N. Dörfliger (2009), Modelling the hydrologic functions of a karst aquifer under active water management—The Lez spring, *J. Hydrol.*, *365*(3–4), 235–243.

Ford, D. C., and P. W. Williams (2007), *Karst Hydrogeology and Geomorphology*, Wiley, Chichester, U. K.

Gerner, A., N. Schütze, and H. Schmitz (2012), Portrayal of fuzzy recharge areas for water balance modelling—A case study in northern Oman, *Adv. Geosci.*, *31*, 1–7.

Goldscheider, N. (2003), Karst groundwater vulnerability mapping: Application of a new method in the Swabian Alb, Germany, *Hydrogeol. J.*, *13*(4), 555–564, doi:10.1007/s10040-003-0291-3.

Gunkel, A., and J. Lange (2011), New insights into the natural variability of water resources in the Lower Jordan River Basin, *Water Resour. Manage.*, *26*(4), 963–980, doi:10.1007/s11269-011-9903-1.

Gupta, H. V., H. Kling, K. K. Yilmaz, and G. F. Martinez (2009), Decomposition of the mean squared error and NSE performance criteria: Implications for improving hydrological modelling, *J. Hydrol.*, *377*(1–2), 80–91, doi:10.1016/j.jhydrol.2009.08.003.

Hartmann, A., J. Lange, M. Weiler, Y. Arbel, and N. Greenbaum (2012), A new approach to model the spatial and temporal variability of recharge to karst aquifers, *Hydrol. Earth Syst. Sci.*, *16*(7), 2219–2231, doi:10.5194/hess-16-2219-2012.

Hartmann, A., J. A. Barberá, J. Lange, B. Andreo, and M. Weiler (2013a), Progress in the hydrologic simulation of time variant recharge areas of karst systems—Exemplified at a karst spring in Southern Spain, *Adv. Water Resour.*, *54*, 149–160, doi:10.1016/j.advwatres.2013.01.010.

Hartmann, A., et al. (2013b), Process-based karst modelling to relate hydrodynamic and hydrochemical characteristics to system properties, *Hydrol. Earth Syst. Sci.*, *17*(8), 3305–3321, doi:10.5194/hess-17-3305-2013.

Hartmann, A., N. Goldscheider, T. Wagener, J. Lange, and M. Weiler (2014), Karst water resources in a changing world: Review of hydrological modeling approaches, *Rev. Geophys.*, doi:10.1002/2013RG000443, in press.

Heilman, J. L., M. E. Litvak, K. J. McInnes, J. F. Kjelgaard, R. H. Kamps, and S. Schwinning (2014), Water-storage capacity controls energy partitioning and water use in karst ecosystems on the Edwards Plateau, Texas, *Ecohydrology*, *7*(1), 127–138, doi:10.1002/eco.1327.

Hirabayashi, Y., R. Mahendran, S. Koirala, L. Konoshima, D. Yamazaki, S. Watanabe, H. Kim, and S. Kanae (2013), Global flood risk under climate change, *Nat. Clim. Chang.*, *3*(9), 816–821, doi:10.1038/nclimate1911.

IPCC (2007), Summary for Policymakers, in *Climate Change 2007: Impacts, Adaptation and Vulnerability. Contribution of Working Group II to the Fourth Assessment Report of the Intergovernmental Panel on Climate Change*, edited by M. L. Parry et al., pp. 7–22, Cambridge Univ. Press, Cambridge, U. K.

Ireson, A. M., and A. P. Butler (2013), A critical assessment of simple recharge models: Application to the UK Chalk, *Hydrol. Earth Syst. Sci.*, *17*(6), 2083–2096, doi:10.5194/hess-17-2083-2013.

Jocson, J. M. U., J. W. Jenson, and D. N. Contractor (2002), Recharge and aquifer response: Northern Guam Lens Aquifer, Guam, Mariana Islands, *J. Hydrol.*, *260*(1–4), 231–254, doi:10.1016/s0022-1694(01)00617-5.

Jukic, D., and V. Denic-Jukic (2009), Groundwater balance estimation in karst by using a conceptual rainfall-runoff model, *J. Hydrol.*, *373*(3–4), 302–315.

Kirchner, J. W., and C. Neal (2013), Universal fractal scaling in stream chemistry and its implications for solute transport and water quality trend detection, *Proc. Natl. Acad. Sci. U. S. A.*, *110*(30), 12,213–12,218, doi:10.1073/pnas.1304328110.

Klemeš, V. (1986), Dilettantism in hydrology: Transition or destiny, *Water Resour. Res.*, *22*(9), 177S–188S.

Kuczera, G., and M. Mroczkowski (1998), Assessment of hydrologic parameter uncertainty and the worth of multiresponse data, *Water Resour. Res.*, *34*(6), 1481–1489.

Lange, J., Y. Arbel, T. Grodek, and N. Greenbaum (2010), Water percolation process studies in a Mediterranean karst area, *Hydrol. Processes*, *24*(13), 1866–1879.

Le Moine, N., V. Andréassian, and T. Mathevet (2008), Confronting surface- and groundwater balances on the La Rochefoucauld-Touvre karstic system (Charente, France), *Water Resour. Res.*, *44*, W03403, doi:10.1029/2007WR005984.

Mangin, A. (1974), Contribution a' l'étude hydrodinamique des aquiferes karstiques: DES thesis, *Ann. Spéléolog.*, *29*(3), 283–332.

Marín, A. I. (2009), The application of GIS to evaluation of resources and vulnerability to contamination of carbonated aquifer. Test site Alta Cadena (Málaga province), MSc thesis, Univ. of Málaga, Malaga, Spain.

Martín-Algarra, M. (1987), Evolución geológica alpina del contacto entre las Zonas Internas y Externas de la Cordillera Bética, PhD thesis, Univ. of Granada, Granada, Spain.

Martínez-Santos, P., and J. M. Andreu (2010), Lumped and distributed approaches to model natural recharge in semiarid karst aquifers, *J. Hydrol.*, *388*(3–4), 389–398.

Milly, P. C. D., K. A. Dunne, and A. V. Vecchia (2005), Global pattern of trends in streamflow and water availability in a changing climate, *Nature*, *438*(7066), 347–350, doi:10.1038/nature04312.

Moore, R. J. (2007), The PDM rainfall-runoff model, *Hydrol. Earth Syst. Sci.*, *11*(1), 483–499, doi:10.5194/hess-11-483-2007.

Mudarra, M. (2012), Importancia relativa de la zona no saturada y zona saturada en el funcionamiento hidrogeológico de los acuíferos carbonáticos. Caso de la Alta Cadena, sierra de Enmedio y área de Los Tajos (provincia de Málaga), PhD thesis, Univ. of Malaga, Malaga, Spain.

Mudarra, M., and B. Andreo (2011), Relative importance of the saturated and the unsaturated zones in the hydrogeological functioning of karst aquifers: The case of Alta Cadena (Southern Spain), *J. Hydrol.*, *397*, 263–280.

Mudarra, M., B. Andreo, A. I. Marín, I. Vadillo, and J. A. Barberá (2014), Combined use of natural and artificial tracers to determine the hydrogeological functioning of a karst aquifer: The Villanueva del Rosario system (Andalusia, southern Spain), *Hydrogeol. J.*, *22*, 1027–1039, doi:10.1007/s10040-014-1117-1.

Peyre, Y. (1974), Géologie dÇAntequera et de sa région (Cordillères Bétiques, Espagne), PhD thesis, Univ. of Paris, Paris.

Plummer, L. N., E. Busenberg, J. B. McConnell, S. Drenkard, P. Schlosser, and R. L. Michel (1998), Flow of river water into a Karstic limestone aquifer. 1. Tracing the young fraction in groundwater mixtures in the Upper Floridan Aquifer near Valdosta, Georgia, *Appl. Geochem.*, *13*(8), 995–1015, doi:10.1016/s0883-2927(98)00031-6.

Rimmer, A., and Y. Salingar (2006), Modelling precipitation-streamflow processes in karst basin: The case of the Jordan River sources, Israel, *J. Hydrol.*, *331*, 524–542.

Samuels, R., A. Rimmer, and P. Alpert (2009), Effect of extreme rainfall events on the water resources of the Jordan River, *J. Hydrol.*, *375*, 513–523.

Samuels, R., A. Rimmer, A. Hartmann, S. Krichak, and P. Alpert (2010), Climate change impacts on Jordan river flow: Downscaling application from a regional climate model, *J. Hydrometeorol.*, *11*(4), 860–879, doi:10.1175/2010JHM1177.1.

Scanlon, B., R. Healy, and P. Cook (2002), Choosing appropriate techniques for quantifying groundwater recharge, *Hydrogeol. J.*, *10*(1), 18–39.

Schmidt, S., T. Geyer, J. Guttman, A. Marei, F. Ries, and M. Sauter (2014), Characterisation and modelling of conduit restricted karst aquifers—Example of the Auja spring, Jordan Valley, *J. Hydrol.*, *511*, 750–763, doi:10.1016/j.jhydrol.2014.02.019.

Seiler, K. P., and J. R. Gat (2007), *Groundwater Recharge From Run-Off and Infiltration*, Springer, Dordrecht, Netherlands.

Sheffer, N. A., M. Cohen, E. Morin, T. Grodek, A. Gimburg, E. Magal, H. Gvirtzman, M. Nied, D. Isele, and A. Frumkin (2011), Integrated cave drip monitoring for epikarst recharge estimation in a dry Mediterranean area, Sif Cave, Israel, *Hydrol. Processes*, *25*(18), 2837–2845, doi:10.1002/hyp.8046.

Son, K., and M. Sivapalan (2007), Improving model structure and reducing parameter uncertainty in conceptual water balance models through the use of auxiliary data, *Water Resour. Res.*, *43*, W01415, doi:10.1029/2006WR005032.

Vrugt, J. A., H. V. Gupta, W. Bouten, and S. Sorooshian (2003), A Shuffled Complex Evolution Metropolis algorithm for optimization and uncertainty assessment of hydrologic model parameters, *Water Resour. Res.*, *39*(8), 1201, doi:10.1029/2002WR001642.

Wood, W. W., and W. E. Sanford (1995), Chemical and isotopic methods for quantifying ground-water recharge in a regional, semiarid environment, *Ground Water*, *33*(3), 458–468, doi:10.1111/j.1745–6584.1995.tb00302.x.

Zagana, E., P. Tserolas, G. Floros, K. Katsanou, and B. Andreo (2011), First outcomes from groundwater recharge estimation in evaporate aquifer in Greece with the use of APLIS method, in *Advances in the Research of Aquatic Environment*, edited by N. Lambrakis, G. Stournaras, and K. Katsanou, pp. 89–96, Springer, Berlin.